Published in : Advanced Science News (2018), 1701059
DOI: 10.1002/adhm.201701059
Status : Postprint (Author's version)

ATMOSPHERIC PLASMA DEPOSITION OF METHACRYLATE LAYERS CONTAINING CATECHOL/QUINONE GROUPS: AN ALTERNATIVE TO POLYDOPAMINE BIOCONJUGATION FOR BIOMEDICAL APPLICATIONS

Urszula Czuba

Materials Research and Technology Department, Luxembourg Institute of Science and Technology (LIST), L-4422 Belvaux, Luxembourg – Chemistry Department, Center for Education and Research on Macromolecules (CERM), CESAM Research Unit, University of Liege, 4000 Liège, Belgium.

Robert Quintana*

Materials Research and Technology Department, Luxembourg Institute of Science and Technology (LIST), L-4422 Belvaux, Luxembourg.

Marie-Claire De Pauw-Gillet*

Mammalian Cell Culture Laboratory—GIGA-R, University of Liege, 4000 Liège, Belgium.

Maxime Bourguignon

Chemistry Department, Center for Education and Research on Macromolecules (CERM), CESAM Research Unit, University of Liege, 4000 Liège, Belgium – Symbiose Biomaterials s.a., 4000 Liège, Belgium.

Maryline Moreno-Couranjou

Materials Research and Technology Department, Luxembourg Institute of Science and Technology (LIST), L-4422 Belvaux, Luxembourg.

Michael Alexandre,

Symbiose Biomaterials s.a., 4000 Liège, Belgium.

Christophe Detrembleur

Chemistry Department, Center for Education and Research on Macromolecules (CERM), CESAM Research Unit, University of Liege, 4000 Liège, Belgium.

Patrick Choquet

Materials Research and Technology Department, Luxembourg Institute of Science and Technology (LIST), L-4422 Belvaux, Luxembourg.

Abstract. Bioconjugation of enzymes on coatings based on polydopamine (PDA) layers is an appealing approach to control biological responses on biomedical implant surfaces. As alternative to PDA wet deposition, a fast, solvent-free, and dynamic deposition approach based on atmospheric-pressure plasma dielectric barrier discharge process is considered to deposit on metallic surfaces

Published in : Advanced Science News (2018), 1701059
DOI: 10.1002/adhm.201701059
Status : Postprint (Author's version)

acrylic-based interlayers containing highly chemically reactive catechol/quinone groups. A biomimetic approach based on covalent immobilization of Dispersin B, an enzyme with antibiofilm properties, shows the bioconjugation potential of the novel plasma polymer layers. The excellent antibiofilm activity against *Staphylococcus epidermidis* is comparable to the PDA-based layers prepared by wet chemical methods with slow deposition rates. A study of preosteoblastic MG-63 human cell line viability and adhesion properties on plasma polymer layers demonstrates early interaction required for biomedical applications.

Keywords. Dispersin B, implant, plasma polymer, polydopamine, surface functionalization.

1. Introduction

Polymer coatings, often in the form of very thin films, have been attracting large attention on the development of biomaterials for the healthcare application. Their ability to control and steer biological–biomaterial interactions as desirable cell responses (adhesion, proliferation, and differentiation) or inhibition of bacteria adhesion has been explored on surfaces of medical devices and implants.[1] The outermost surface layer of the coating is critical on governing both the biological responses and biomechanical environment. In the latest decades, immobilization of biomolecules to control the adsorption of proteins and adhesion of bacteria on the outermost surface has developed rapidly. Indeed, this fast development has taken advantage of the well-known enzyme immobilization technologies, for instance, for the production of polysaccharides, amino acids, and pharmaceutical products, already available industrially.[2] Polydopamine (PDA) coatings have shown to be a promising approach for the biofunctionalization of implant surfaces.[3] The coating is very resistant and allows easy functionalization through catechol chemistry.[4] Enzymes can be covalently immobilized on PDA coatings via Michael addition and Schiff-base reactions with protein functional groups (thiol, amine, and imidazole).[5] Self-polymerization of dopamine by well-known wet chemistry methods is currently the most common approach to prepare PDA coatings. One of the main limitations of this process is however the slow deposition rate. In addition, PDA coating is deposited by immersion of the object in the solution, which generates huge amount of waste. An alternative approach, also by means of wet chemistry, is the deposition of polymers bearing catechol units from aqueous or organic solutions.[4,6] However, these catechol-containing coatings are mainly produced by multistep procedures.

Atmospheric-pressure plasma (AP plasma) technology is engaging attention as solvent-free, single-step surface modification method of biomaterials.[7] In the field of biomedical application, three main approaches have emerged: direct therapy, surface modification, and plasma deposition. AP plasmas for direct therapy have shown to kill cells selectively without damaging the surrounding area.[8] As a surface treatment, AP plasmas have shown their versatility toward formation of reactive species for surface activation and functionalization. Through oxidation, etching or attachment of chemical groups, surface physical and chemical properties have been modified.[9] Plasma technology has already been applied on the deposition of functional polymeric layers on surfaces of metallic and polymeric implants.[7b,c,10] Particularly, bioconjugation has been mainly conducted on plasma-polymerized

Published in : Advanced Science News (2018), 1701059
DOI: 10.1002/adhm.201701059
Status : Postprint (Author's version)

coatings with acid, amine, epoxy, and alcohol functionalities.[11] Recently, the plasma copolymerization method allowed the deposition of plasma polymer layers with catechol and quinone functionalities.[11b,12]

Bacteria attachment with biofilm development on a medical implant surface can cause several adverse events, from hampering the wound healing process to cause the failure and loosening of the implant.[13] Staphylococcal infections are one of the most frequent nosocomial infections on indwelling medical devices and implants.[14] As several biofilm-forming bacteria, Staphylococcal biofilms are encased within a protective extracellular matrix formed of exopolysaccharides (EPS).[14a,15] A bioinspired approach to avoid bacteria to adhere and form resistant biofilms is biofilm-dissolving enzymes as those generated by bacteria during sessile growth.[16] An example is Dispersin B (DispB), a ß-*N*-acetylglucosaminidase active against EPS and able to disperse and detach Staphylococcal biofilms.[13,17] DispB has been loaded in polymeric coatings showing biofilm dispersion activity upon release to the media.[17] Recently, Faure et al. reported the bioconjugation of DispB on catechol-containing nanogels prepared by layer-by-layer solution deposition. The biofunctionalized nanogels showed antibiofilm activity against *Staphylococcus epidermidis* with adherent bacteria reductions of 93% in comparison with the nanogel without DispB.[18]

Cellular interactions with various biomaterials (regeneration-guided bone materials, polymers, metallic pieces, or nanoparticles (NPs)) promote the tissue reconstruction. Initial cellular adhesion is first studied and then long-term experiments are needed to proof the sustainability of tissue integration properties. Indeed, long-term implant osseointegration stills a fundamental clinical research field. For instance, in oral pathology, for the bone and the gingival tissue reconstruction, bone regeneration allowing the dental placement of implant has been always regarded as a clinical challenge.[19] Peri-implantitis is caused by bacteria, which develop on a biofilm structure on the lower part of the implant causing resorption of the bone.[20] Investigating osteoblastic responses in vitro is widely used before developing in vivo studies.[21] Human preosteoblastic MG-63 cell line is one of the common interesting cell lines to investigate the osteoblastic response to biomaterials[22] and also to saliva contamination.[23]

In our previous works, we reported on a dynamic deposition approach based on atmospheric-pressure dielectric barrier discharge plasma process for the deposition of catechol and quinone functional groups on stainless steel (SS). There, the liquid-assisted plasma-enhanced chemical vapor deposition (LA-PECVD) technique allowed the deposition, within minutes, of inorganic silane-based layers able to immobilize enzymes as New Delhi metallo-β-lactamase-1 for biotechnological applications.[11b] However, their suitability for the application in the biomedical field was not shown. Indeed, reports of AP plasma technology for the deposition of polymer layers with potential application on implants are scarce. Widely used in biomedicine, methacrylic polymers are characterized by a good stability, chemical passiveness, and mechanical resistance and have been reported to be bio- and cytocompatibles.[24] In this work, aiming at the deposition of fully organic reactive polymeric layers for the biofunctionalization of biomedical metallic surfaces, LA-PECVD was employed to deposit methacrylic-based plasma polymer layers containing quinone/catechol units. After deposition, bioconjugation was carried out by immobilization of DispB. The antibiofilm activity of the surface-functionalized plasma polymer layer was then evaluated and compared against PDA layers produced

Published in : Advanced Science News (2018), 1701059
DOI: 10.1002/adhm.201701059
Status : Postprint (Author's version)

by deposition in solution and functionalized in the same manner. In particular, PDA was considered in this study as reference of catechol-/quinone-rich layers for surface biofunctionalization.[5a,25] Finally, human MG-63 cell viability and adhesion properties on the plasma polymer layers were compared to evaluate their osteoblastic response and suitability for biomedical applications.

2. Results and Discussion

2.1. PLASMA POLYMER LAYER DEPOSITION

The LA-PECVD approach was successfully used for the AP plasma-assisted copolymerization of a L-3,4-dihydroxyphenylalanine (L-DOPA) derivative monomer; methyl DOPA methacrylamide (DOMAm), with ethylene glycol dimethacrylate (EGDMA) as comonomer. The chemical structure of the bioinspired catechol vinyl monomer, DOMAm, is shown in **Figure 1** together with the scheme of the plasma deposition process. EGDMA was required to solubilize DOMAm that is in solid form. The use of coprecursors is usually employed by CVD techniques to process nonvolatile monomers. For this study, a bifunctional monomer was preferred to prepare functional plasma polymer layers stable in aqueous physiologic medium. Polyvinyl monomers are commonly used as crosslinkers, thus expected to promote more resistant polymer layers by formation of a crosslinked matrix layer. DOMAm concentration in the feed mixture was kept constant at 0.007 mmol·mL^{-1}, which was determined experimentally to be near the solubility saturation point at room temperature. The dependence of layer thickness of the plasma polymerization of EGDMA/DOMAm mixture in function of the number of deposition cycles is shown in Figure 1c. An average dynamic deposition rate of 21 nm·m min^{-1} was calculated from the curve and moving table speed. At a higher number of cycles (>300), film growth seemed to stabilize. This effect was suspected to be consequence of the heating up of the moving table, which might increase the evaporation of sprayed liquid layer. Deposition cycles to prepare the functional layers were then limited to up to 200 cycles. The deposited layers showed good thickness homogeneity (±5% of average thickness).The longitudinal speed of the deposition-moving table, kept constant at 100 mm·min^{-1}, allowed preparing submicrometer plasma polymer layers within few minutes. This time scale to prepare the plasma layers is remarkably different from the solution deposition of PDA layers that generally takes place within hours.[4,5] In addition, under the selected conditions, plasma layers were produced using only few microliters of solutions, contrary to the large volume of solution generally used for PDA wet deposition.[4] The plasma deposition

was also carried out successfully on rough surfaces, as those of chemical-etched titanium (Figure S1, Supporting Information). Indeed, the configuration of the plasma reactor will allow the deposition on surfaces with roughness or pattern features of few dozen of micrometers without formation of plasma heterogeneities.

Published in : Advanced Science News (2018), 1701059
DOI: 10.1002/adhm.201701059
Status : Postprint (Author's version)

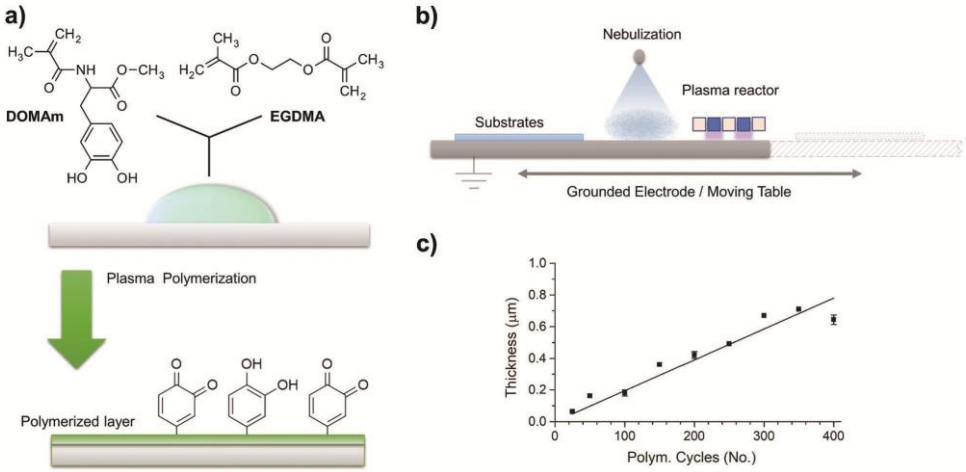

Figure 1. Schematic representation of the deposition of polymethacrylate-based bioinspired layers containing catechol/quinone moieties a) and b) LA-PECVD set-up used for the deposition process. Thickness versus number of polymerization cycles c) on the plasma deposition of EDGMA/ DOMAm mixtures. Means ± SD (*n* = 6) for 100, 200, and 300 polymerization cycles.

2.2. PLASMA LAYER CHARACTERIZATION AND STABILITY

As deposited plasma polymer layers were able to completely cover disc sample surface with a polymer coating-like visual appearance (different from characteristic oily aspect of unpolymerized layers), in which adhesion to the surface was confirmed by peeling tests. Retention of the functional groups' characteristic of the polymers was confirmed in all deposited layers by microscope grazing angle Fourier-transform infrared (FTIR) analysis (Figure S2, Supporting Information). Strong ester carbonyl stretch at 1720–1730 cm^{-1} and C–O–C stretching vibration from 1150 to 1300 cm^{-1} indicate the retention of ester groups in the deposited films. In addition, strong vibration of the α-methyl group at 1380 and 1454 cm^{-1} bending vibration of C–H bonds of the $–CH_3$ group was observed. The formation of hydroxyl groups by scission of ester methoxy groups from methacrylate might be the origin of the absorbance bands observed at 3500–3300 cm^{-1} range of the FTIR spectra.[26] Presence of absorption bands from DOMAm units was not detectable on the plasma layers. The chemical composition of the plasma polymer layer was analyzed by X-ray photon spectroscopy (XPS) analysis, and the atomic percentages calculated from the high resolution spectra are summarized in **Table 1**. Considering the composition of plasma layers prepared from neat EDGMA, i.e., without DOMAm, in addition to expected C and O atoms, the presence of small amount of nitrogen was detected. Angle-resolved XPS measurements confirmed the distribution of nitrogen was constant through the first 10 nm of the plasma layers. Therefore, the presence of nitrogen was considered to be consequence of the incorporation of nitrogen from the ambient through reaction with plasma.[26] The open configuration of the plasma reactor might promote such occurrence. In addition, the potential participation of dissolved air in the sprayed liquid films could not be neglected. Despite the weak signal and interference of the external nitrogen incorporation, the presence of nitrogen ascribed to the secondary amide of DOMAm in plasma layers prepared from EGDMA/DOMAm mixtures was evidenced by the

Published in : Advanced Science News (2018), 1701059
DOI: 10.1002/adhm.201701059
Status : Postprint (Author's version)

peak at ≈399 eV (NH-C=O) on XPS N1s spectra (Figure S3, Supporting Information). It is worth noting that nitrogen atomic percentage in the EGDMA/DOMAm mixture feed is 0.01%, below the quantification limits of XPS technique. The estimated higher nitrogen concentration ascribed to DOMAm in the layers indicated the occurrence of EGDMA evaporation during the deposition process.

Plasma polymer layers showed C/O ratios significantly below the theoretical value of 2.5. This trend is opposite to reported increase of C/O ratio on gas phase plasma-polymerized methacrylates as PMMA, either in vacuum or at atmospheric pressure.[26,27] Increase of C/O ratio has been ascribed to the scission of the ester methoxy groups and formation of C□O or O□C□O groups. We interpret the lower C/O ratios as consequence of presence of DOMAm units and the participation of oxygen from atmospheric air. The increase in oxygen content will support the significant increase of hydrophilicity of the plasma EDGMA layers with values of water contact angle (WCA) about 20% lower than conventional PMMA surfaces. Formation of oxygen-containing polar groups is commonly attributed to the decrease in WCAs of PMMA exposed to oxygen plasmas.

Table 1. XPS atomic percentage composition of plasma polymer and PDA layers.

Layer	XPS [At%][a)]			
	C	O	N	C/O
Poly(EGDMA) (theoretical)	71.4	28.6	0.0	2.5
pPoly(EGDMA)	65.5	34.0	0.5	1.9
pPoly(EGDMA-*co*-DOMAm)	62.3	37.1	0.6	1.7
pPoly(EGDMA-*co*-DOMAm) + DispB	65.3	22.6	12.1	2.9
PDA	69.1	23.7	7.2	2.9
PDA + DispB	65.7	22.7	11.6	2.9
DispB (theoretical)	63.3	19.3	17.4	3.3

[a)]Polymer plasma layer atomic composition determined by XPS, based on C, O, and N contents only.

The optical absorption and fluorescence properties of chromophore catechol/quinone groups were exploited to further evidence the presence of these reactive moieties on the plasma polymer layer. In **Figure 2**a, the UV absorption spectra of the pPoly(EGDMA) and pPoly(EGDMA-*co*-DOMAm) layers are shown. The presence of a narrow peak at 260 nm is observed in the absorption spectrum of pPoly(EGDMA-*co*-DOMAm) layer and is attributed to the presence of catechol groups.[6] The broader absorption band, centered at 450 nm, which is not present on pPoly(EGDMA) spectrum, is likely to be related to quinone groups.[11b] Confocal fluorescence microscopy was conducted at the excitation wavelength of 405 nm, allowing the detection of catechol/quinone moieties and visual assessment of their distribution in the layer surface. For the sake of comparison, fluorescence images showed in Figure 2b are side-byside observations of two disc samples coated with plasma layers with and without DOMAm incorporation. Despite the SS background auto-fluorescence, the distribution of the fluorescence was found to be uniform and considered to be originated by the catechol/quinone moieties present in the layers. As a control assay, the deposition of plasma pPoly(EGDMA) on indium

Published in : Advanced Science News (2018), 1701059
DOI: 10.1002/adhm.201701059
Status : Postprint (Author's version)

tin oxide (ITO) glass, which do not present the background fluorescence phenomena, was also conducted and no fluorescence was measured (data not shown).

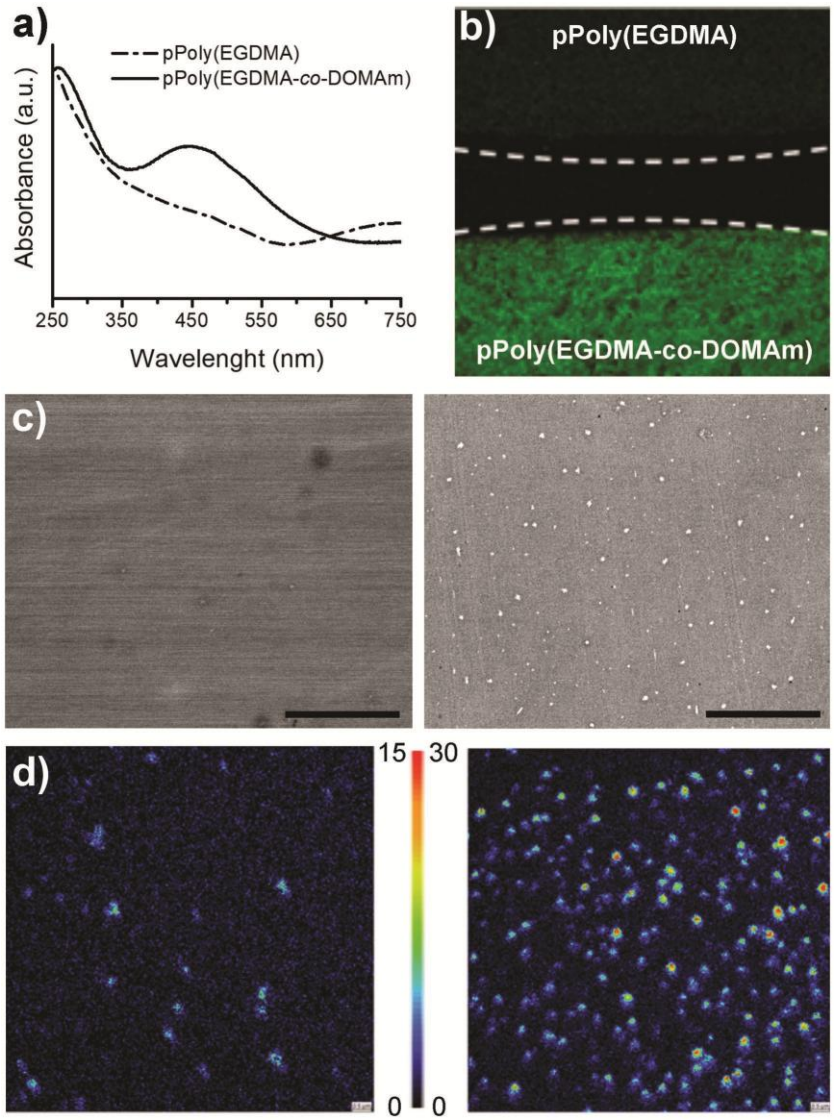

Figure 2. Confirmation of catechol/quinone groups in polymer plasma layers containing DOMAm units. a) UV–vis absorption spectra. b) Fluorescent confocal microscopy image of two disc samples observed side-by-side (dashed lines to help indicate disc sample borders). c) SEM images of layers after immersion in $AgNO_3$ solutions (scale bar 10 µm) and d) NanoSIMS mapping of silver (10 × 10 µm).

The presence of catechol/quinone groups at the layer topmost surface is critical for the bioconjugation. The upmost layer of the plasma layer was investigated using the catechol redox chemistry by immersion in a silver ($AgNO_3$) solution, followed by scanning electronic microscopy (SEM) observation of silver NPs generated by oxidation of catechol moieties. The immobilization of silver NPs on the surface is promoted by stabilizing bonds involving both catechol and quinone functional groups.[18] SEM analyses (Figure 2c) revealed the presence of numerous NPs, in which silver nature was confirmed through energy dispersive X-ray spectroscopy (EDX) analysis showing peaks at 3 and 3.2

Published in : Advanced Science News (2018), 1701059
DOI: 10.1002/adhm.201701059
Status : Postprint (Author's version)

keV. The SEM images of the immobilized NPs indicate a rather uniform distribution of the catechol groups on the surface of plasma pPoly(EDGMA-*co*-DOMAm) layer. Complementary to EDX analysis, nanoscale secondary ion mass spectrometry (NanoSIMS) analyses were carried out. NanoSIMS allows for sub-micrometer elemental and isotopic characterization of materials with a lateral resolution of 150 nm.[28] In Figure 2d, the NanoSIMS silver mapping images are shown for plasma polymer layers with and without DOMAm units. Absorption of silver on net plasma pPoly(EDGMA) is observed but with a significant less intensity.

Stability of the polymer plasma layers was assessed by incubation in phosphate buffered saline (PBS) solution 10×10^{-3} m at pH 5.9 and 8. This pH range has been commonly utilized on biomolecule grafting studies of PDA-based coatings.[5a,6,18] For these stability assays, thick plasma layers, i.e., 500–600 nm were considered to reduce the experimental error on the measurement of weight difference before and after immersion. **Figure 3**a shows the evolution of relative remaining weight of studied plasma layers after immersion to up to 60 min. The plasma layers showed a significant stability in terms of remaining weight after immersion tests in PBS. To illustrate the surface preparation, complementary surface observations were done by atomic force microscopy (AFM) on coated samples before and during immersion. Figure 3b shows the topographic scan images and height profiles that reveal significant changes in the surface topography and roughness. In dry condition, the surface is smooth and uniform, where in PBS buffer topographical features in form of bumps are visible. Despite these features, the average step-high values obtained for the layer in air and PBS were not significantly different as revealed the height profiles. The formation of the bumps was found to be reversible; after rinsing the surface with water, nitrogen blow drying and measuring again in dry condition, no apparent changes in the morphology and thickness were found. The occurrence of significant loss or delamination of the layers from the SS substrates was therefore dismissed. Consequently, the bumps observed were interpreted as bubbles originated by local detachment of the layer from the mirror-polished SS substrate.

Published in : Advanced Science News (2018), 1701059
DOI: 10.1002/adhm.201701059
Status : Postprint (Author's version)

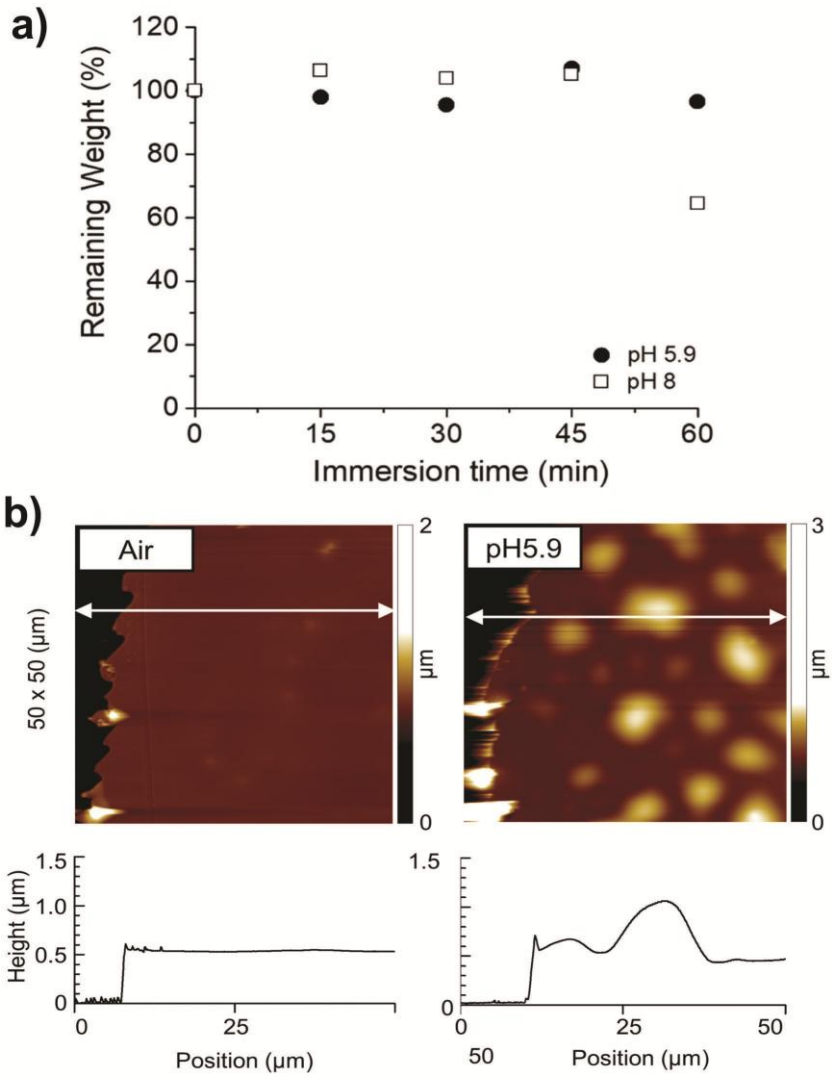

Figure 3. Stability of the polymer plasma layers in PBS buffer a) and b) morphology AFM images (50 × 50 µm) with height profile of scratched pPoly(EDGMA-*co*-DOMAm) layers in dry and liquid conditions.

2.3. BIOMOLECULE GRAFTING AND ANTIBIOFILM PERFORMANCE

An encouraging motivation for the preparation of methacrylate-based plasma polymer layers is their high potential to form biocompatible layers on metal surfaces relevant for clinical applications. SS is often used for temporary implants (bone fixation, screws, prostheses, catheters, and orthodontics) whether titanium alloys are considered for long-term implants. The success of the further biofunctionalization of these methacrylic plasma layers prepared by copolymerization with DOMAm will rely on the capability of the very reactive catechol/quinone groups for binding biomolecules. Targeting the prevention of Staphylococcal biofilms formation, the immobilization of DispB was conducted. DispB is an enzyme well known to be active against *S. epidermidis* biofilm forming.[17,29] Specifically, a bioengineered similar of DispB bearing an uncleavable hexahistidine (His6) tag was selected for this study. The grafting step was conducted at pH 7.2, where histidine (pKa ≈ 6) tags are

Published in : Advanced Science News (2018), 1701059
DOI: 10.1002/adhm.201701059
Status : Postprint (Author's version)

suitable for covalent binding through reaction with quinone groups. DispB immobilization was conducted on both PDA and plasma polymer layers.

In order to verify the successful immobilization of the enzyme, samples surface was characterized by XPS before and after the grafting step, which was followed by thorough cleaning to remove unbounded enzyme. Summarized on Table 1, the nitrogen atomic content on the grafted surface was found to be increased by more than tenfold from 1% to 12% because DispB has a higher nitrogen content compared with one of the plasma layers, indicating the presence of the biomolecule on the surface. Indeed, the chemical composition measured by XPS of the plasma layer (approximately the topmost 5 nm) after immobilization approaches to the theoretical atomic composition of DispB. The antibiofilm activity against *S. epidermidis* formation of the grafted biomolecules on plasma polymer and PDA layers was assessed using plasma-cleaned SS discs as control. PDA layers deposited on SS discs were used as a reference of a well-documented catechol/ quinone-rich layer for biomedical applications.[30] After 24 h of incubation, bacteria growth (adherent and nonadherent) on surfaces was found only slightly affected by the surface treatment. Prior to biomolecule immobilization, surfaces coated with the PDA presented significantly higher bacterial amount than both plasma polymer layer and plasma-cleaned SS control surface. Bacterial adhesion on PDA surface was interpreted as a consequence of the expected higher catechol/quinone units on the surface, which have been reported to favor bacteria attachment.[31] In contrast, clear differences were observed (**Figure 4**) for the layers with immobilized DispB with adherent bacteria reductions of nearly 90% for both plasma polymer and PDA layers, indicating a very high antibiofilm performance. This result also confirms that the immobilization of DispB on the surface was conducted with retention of the enzymatic activity. Furthermore, the antibacterial adhesion performance on the bioactivated plasma layers suggests that the bounding to the surface might occur through reaction of quinone groups with imidazole groups in the His6 tag. Interesting, the antibacterial formation performance obtained in this study against Gram-positive *S. epidermidis* is very similar to the one previously reported on PDA-based nanogels functionalized with DispB.[18] In addition, on that study, the antibacterial activity was also found to be very high against Gram-negative bacteria (*Escherichia coli*).

Published in : Advanced Science News (2018), 1701059
DOI: 10.1002/adhm.201701059
Status : Postprint (Author's version)

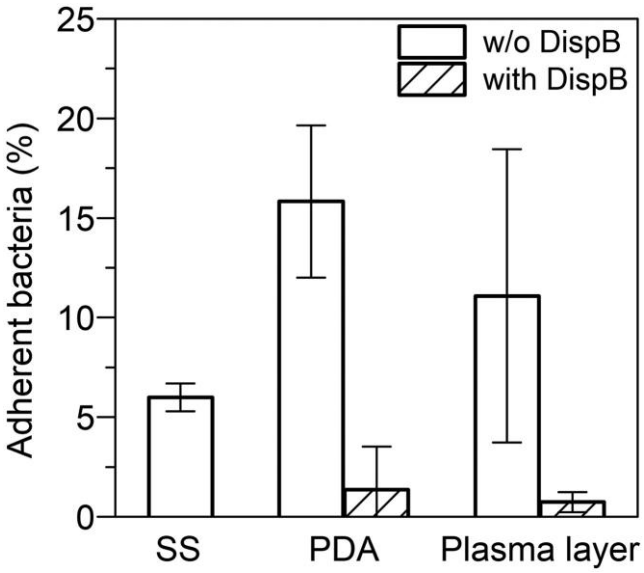

Figure 4. Antibiofilm formation activity comparison between plasma polymer layers and PDA layers deposited on plasma-cleaned SS before and after grafting of DispB. Means ± SD (*n* = 3).

2.4. CELL VIABILITY AND ADHESION ASSAYS

For any medical applications of these biofunctionalized surfaces to prevent biofouling as, for instance, on metallic implants, it is now important to verify that this chemical-modified functional surface is able to limit, in short-term implants, or to promote, in long-term implants, cell adhesion, migration, proliferation, and differentiation. As for bacteria assays, first steps of interactions with functionalized surfaces were investigated. For that, preosteoblastic MG-63 cell viability and adhesion properties on DispB-grafted plasma polymer surfaces were carried out as indicators of their later osseointegration potential. Cell metabolic activity was first evaluated by [3-(4,5-dimethylthiazol-2-yl)-5-(3carboxymethoxyphenyl)-2-(4-sulfophenyl)-2H-tetrazolium inner salt (MTS) assays on PDA and pPoly(EGDMA-*co*-DOMAm) layers with and without DispB immobilization (**Figure 5**a). Statistical comparison using Mann Whitney tests revealed that the presence of DispB on the surfaces does not add a significant effect on cell viability ($P > 0.05$). With regard to plasma-cleaned SS disc controls taken as 100%, cell viability was found to be reduced on all coated surfaces, with absorbance diminution up to 58% for the bioactivated plasma layer. This lower viability was in agreement with immunofluorescence microscopy results after dual staining with (4′,6-diamidino-2-phenylindole dihydrochloride) DAPI for nuclei and phalloidin for actin filaments at 72 h (Figure 5b,c). Microscopic fluorescent images' quantitative analyses revealed lower cell number and percentage of surface occupied by cells on plasma polymer-coated surfaces. WCAs of both the plasma polymer and PDA layers, 52.3 ± 2.7 and 54.7 ± 2.0, respectively, were considered adequate for cell attachment.[32] In all conditions, the occupancy of surface was quite homogeneous, but some areas with low number of cells were observed, which may be due to irregular cell attachment/detachment, migration, spreading, and growth. Less spread phenotypes were evidenced in these areas. In confluent areas, no growth as aggregates could be observed. The immobilization of DispB on plasma polymer layers seems to reduce

Published in : Advanced Science News (2018), 1701059
DOI: 10.1002/adhm.201701059
Status : Postprint (Author's version)

the number of cells up to 20% in comparison to plasma-cleaned SS controls (Figure 5b). Donelli et al. assessed the cytotoxicity of DispB toward Hep-2 cells reporting no significant changes in the general morphology of the monolayer or in the major cytoskeletal components (F-actin and α- and β-tubulins).[17] The observed effect was interpreted on context of cell/surface interactions rather than DispB toxic effect. Morphological analyses showing no sign of cellular suffering supported this hypothesis. Percentages of cell spreading calculated on the surfaces were not significantly modified (Mann– Whitney test, $P > 0.05$) (Figure 5d). The difference observed on plasma layers between adhesion properties of osteoblast cells could agree with the reported studies.[21b,33] Cell attachment has been reported to be more sensitive to surface energy whether spreading seems to be more influenced by the chemistry of the surface.[34] Cell images on each surface are shown in **Figure 6**. Elongated cells with thin cytoplasmic expansions (osteoblasticlike phenotype) were observed (see higher magnification images in Figure S4, Supporting Information). Numerous filopodiamediated contacts between cells and between cells and substrate were evidenced using actin fluorescent marker. Vinculin was positive in the cytosol (**Figure 7**a). This set of results clearly indicates that despite the observed lower cell attachment results on plasma polymer layers, the potential osseointegration properties are interesting to test for long-term implant stability, to evaluate whether they will be compromised. Indeed, cell attachment follows the trend observed on bacteria adhesion results before DispB conjugation; where bacteria were more adherent on PDAcoated surfaces than on the plasma layer. In both cases, biofunctionalized surfaces are more selective toward cell attachment rather than bacteria biofilm forming, further demonstrating the potential of the plasma layer as alternative to PDA coatings for implant surfaces.

In a final case study to assess the potential application of the pPoly(EGDMA-*co*-DOMAm) layers on permanent implants, chemical-etched titanium (dental implant grade) was used as a model surface. On plasma polymer-coated surfaces, MTS assays revealed cell viability of 82%, only slightly below than on uncoated titanium. The viability percentages are above 70%, which is considered as noncytotoxic. Interestingly, morphological analysis showed spreading increase on coated surface (Figure 7b). In comparison with mirror-polished SS surfaces, the higher osseointeraction observed might be related to the roughness of etched titanium surface.[19,35] Surface topography has a high impact on cell behavior. Generally, it increases proliferation of cells, for instance, in titanium dental implants.[36] In implantology, titanium is a gold standard material in gingival-level implants.[37] The osseointegration of oral implants is related to the early interaction between osteoblastic cells and titanium surface.[21a] The surface roughness plays a critical role in early cell adhesion, spreading, proliferation, and differentiation. The results on SS and etched titanium might indicate that osseointegration of bioconjugated plasma polymer layers would be slightly reduced at the same time as bacterial adhesion reduction, but to a lower extend. This would be beneficial for short-term implants. Further investigation on implants with rough titanium surfaces will be required to evaluate the osseointegration potential for long-term implants.

Published in : Advanced Science News (2018), 1701059
DOI: 10.1002/adhm.201701059
Status : Postprint (Author's version)

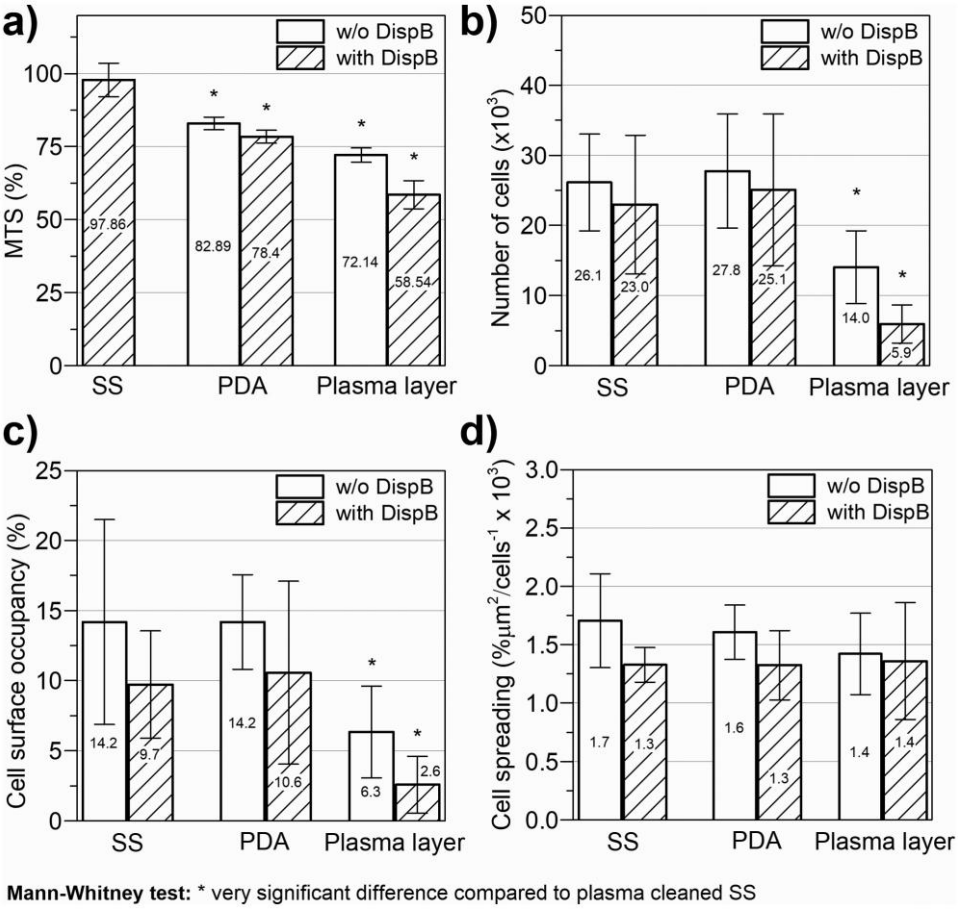

Figure 5. Cellular viability compared with plasma-cleaned SS (100%) a), cell number b), cell coverage c), and cell spreading d) of MG-63 after 72 h of culture on discs. Means ± SD (n = 6) *P value < 0.01 (Mann–Whitney test). 100% cell surface occupancy or cell spreading per disc corresponds to 3.1416 cm^2.

3. Conclusions

Aiming at developing an alternative to PDA coatings for surface bioconjugation, AP plasma deposition was studied for the deposition of functional methacrylic layers containing a bioinspired monomer derived from DOPA. The deposition process characterized by being fast, solvent-free, and highly reliable allowed the preparation of layers with controllable thickness containing active quinone and catechol units uniformly distributed over the layer surface. The bioinspired approach for the biofunctionalization of the layers via immobilization of DispB showed to be successful on the preparation of surfaces with high activity against the adhesion of *S. epidermidis* biofilm. The results of in vitro tests of the plasma pPoly(EGDMA-*co*DOMAm) layers concerning their noncytotoxicity demonstrated that they are suitable for future use in biomedical applications. When considering DispB biofunctionalized surfaces, significant differences were found on the total number of MG-63 cells covering the surface and on surface coverage in the presence of DispB. Cellular assays did reveal some

Published in : Advanced Science News (2018), 1701059
DOI: 10.1002/adhm.201701059
Status : Postprint (Author's version)

differences between the plasma deposition solution and "classical" wet approach using PDA deposition on model smooth SS surface. Remarkably, cell spreading on both surfaces was similar. Evolution with longer times could be interesting to study as well as cocultures with bacteria, in order to compare early and late advantages of antibiofilm formation activity with regard to osteoblastic activity (attachment, spreading, growth, and differentiation). This work paves the way for the use of atmospheric plasma technology as fast deposition method for the production of fully organic-functionalized interlayers, suitable for biomolecule immobilization, with application on the surface treatment of biomedical devices and implants. The method demonstrated here is not limited to 2D but can be transferred to implants, for instance, by using an atmospheric plasma torch (**Figure 8**).

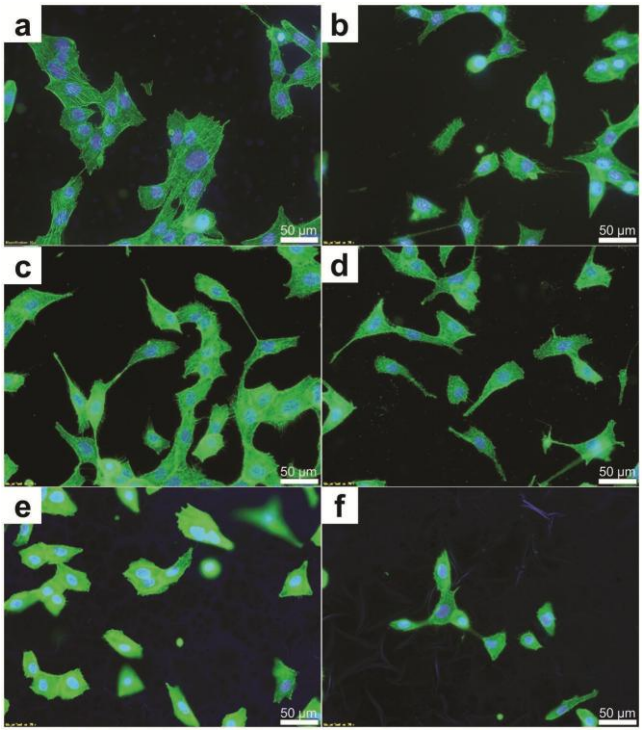

Figure 6. Immunofluorescence microscopy. Dual staining with phalloidin for actin (green) and with DAPI for nuclei (blue) of MG-63 cells after 72 h of culture on discs; Z stacking, IX 81 Olympus microscope, objective 20× (immersion oil): SS a), SS + DispB b), PDA c), PDA + DispB d), plasma layer e) and plasma layer + DispB f).

Published in : Advanced Science News (2018), 1701059
DOI: 10.1002/adhm.201701059
Status : Postprint (Author's version)

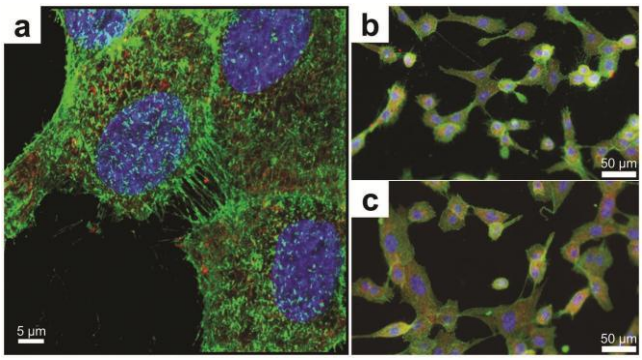

Figure 7. DAPI in nuclei (blue), vinculin in cytoplasm (red), and actin (green) showing filopodia with Microscope confocal Super Resolution Zeiss LSM 800-Airyscan processing (see video in the Supporting Information) on a) SS DispB surface and with Z stacking, IX 81 Olympus microscope (20× objective, immersion oil) on b) etched titanium, and c) etched titanium coated with pPoly(EGDMA-*co*-DOMAm).

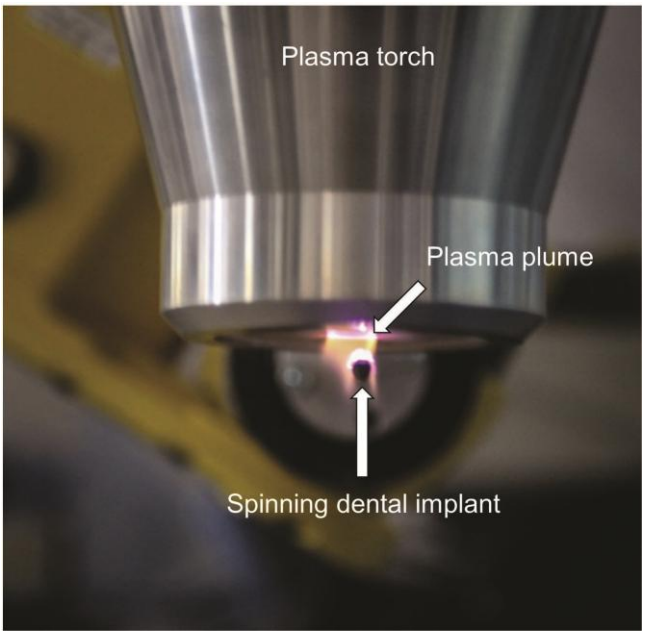

Figure 8. Example of deposition on a dental implant of the plasma layer using an AP plasma torch. Comparable to the deposition process shown in Figure 1b, the implant is moved from the nebulization to the torch zone using a robotic arm that also spins the implant.

4. Experimental Section

Materials: EGDMA (98%) and silver nitrate ($AgNO_3$) were purchased from Sigma-Aldrich and used as received. The DOMAm, methyl 3-(3,4-dihydroxyphenyl)-2-(2-methylprop-2-enamido)propanoate), and DspB (42 kDa with His6 His-Tag) were prepared by Symbiose Biomaterials, Belgium. Mirror-polished SS discs (ø 20 mm, 1 mm thickness) were cut out from 304-8ND SS sheets. After removing the adherent protective film, the discs were cleaned with ethanol and consecutive ultrasonic washing in acetone (three times, 5 min each) and ethanol absolute (three times, 5 min each) before their use to

Published in : Advanced Science News (2018), 1701059
DOI: 10.1002/adhm.201701059
Status : Postprint (Author's version)

eliminate any adhesive residues. Acid-etched titanium discs (ø 10 mm, 2 mm thickness, average roughness of 2 µm) were kindly provided by Nobil Bio Ricerche S.r.l. and cleaned in a similar manner.

LA-PECVD: The LA-PECVD setup used for plasma polymerization was described previously.[12a] Briefly, the system consisted of two electrodes placed in parallel with an active plasma zone of 18.72 cm^2. The moving table was the grounded electrode and two high-voltage horizontal bars (10 kHz sinusoidal electrical excitation—SOFTAL "corona generator 7010R," at power density 1.6 W cm^{-2}) with thick alumina insulation composed the second electrode. Plasma gas was injected though one gas supply bar between the high-voltage bars. Mirror-polished SS disc samples (or etched titanium discs) were placed flat over the moving table with the help of a holder, of the same disc thickness to avoid border effect by maintaining a constant 1 mm gap between the two electrodes. In a first step, the discs were exposed to Ar/O_2 (5% v/v O_2) plasma mixture (20 slm) for ten consecutive runs at table speed of 10 mm s^{-1} to clean/activate the exposed surface (this step was also carried out to prepare the plasma-cleaned control surfaces for the biological assays). Subsequently, the solution of DOMAm in the comonomer was injected with the help of a syringe pump to the feed nebulization system, and the polymer plasma deposition was carried out with an increased speed of 100 mm s^{-1} using 20 slm argon gas (99 999%) plasma. Up to 400 runs were conducted. On each run, the samples were subjected to a liquid deposition step and two transitions by the plasma zone as shown in Figure 1. A venturi-based nebulizer system (VITO) using 2 slm nitrogen nebulization gas and 2 slm nitrogen carrier gas was used to produce a soft, highly focused, fine mist spray. The reproducibility of the setup was determined by measuring the thickness of the deposited layer on samples produced in at least six independent depositions (batches).

PDA Deposition: PDA layers were deposited on SS discs as reported elsewhere.[4] Briefly, the discs, cleaned as previously described, were rinsed with Tris buffer (Tris (CAS 77-86-1) 10×10^{-3} m in deionized water) before placing them vertically, with the aid of a holder, inside a 1 L glass beaker, facing inside and allowing space for the stirrer at the bottom. PDA deposition solution in 10×10^{-3} m Tris buffer (2 mg mL^{-1} dopamine hydrochloride—CAS 62-31-7, equilibrated at pH 8.5 with acid chloride 1 m) was added to beaker. PDA deposition was carried out for 24 h under gentle agitation. After removing the holders from the solution, the discs were rinsed three times with deionized water to remove buffer traces and left to dry before use.

Grafting of Silver NPs (SEM Analysis): Grafting of silver NPs was carried out by surface oxidation of catechols units with silver nitrate. Samples were immersed for 24 h in $AgNO_3$ solution in milliQ water (1 mg mL^{-1}) under agitation. After this period of time, samples were washed five times for 5 min in milliQ water to remove solution traces, blown dried with nitrogen, and analyzed by SEM.

Sample Characterization Methods: Scanning electron microscopy analysis was carried out using field emission microscope Hitachi SEMSU-70 at various points of the surface. Weight change measurements of deposited coatings before and after immersion in PBS buffer at different pH were performed using a Sartorius ME36-S microbalance (+/−2 µg). The samples after immersion were blow dried with nitrogen before weighting. FTIR spectra of coated surfaces were obtained using a Bruker Hyperion 2000 microscope equipped with a grazing angle objective and a MCT detector coupled to IR Bruker Vertex 70 apparatus. The spectra were acquired with 200 scans recorded in 4000–800 cm^{-1} range with resolution of 4 cm^{-1}. XPS analysis was carried out in a Thermo VG Microlab 350 Scanning

Published in : Advanced Science News (2018), 1701059
DOI: 10.1002/adhm.201701059
Status : Postprint (Author's version)

Auger Microscope instrument having a monochromatic Al Kα X-ray source (*h*ν = 1486.6 eV) at a pass energy of 20 eV. Casa XPS program was used to process the XPS spectra. Angle-resolved XPS was carried out at take off angle (TOA) of 0° and 45°. For every batch, three centrally located points per sample were analyzed. UV–vis spectroscopy was conducted using PerkinElmer Lambda 950 UV–vis–NIR spectrophotometer equipped with 100 mm integrating sphere with a PMT/InGaAs detector. The scan range maintained from 750 to 250 nm, PMT below 860 nm, and slit at 2 nm. For every batch, one centrally located point per sample was analyzed. Fluorescence confocal microscopy at excitation wavelength of 405 nm was conducted on a Zeiss LSM 800—Airyscan microscope equipped with GaAsP detector and fast linear scanning. A mechanical profilometer was used to measure the thickness of plasma polymer layers deposited on silicon wafer after scratching. The step-high values of millimeter-long scratches were measured at three different points along the scratch, reporting the average value. AFM measurements were performed with a PicoLE microscope (Molecular Imaging). Images were acquired in air (dry thickness) and in PBS buffer at pH 6 and 8 in AC mode at scan rates between 0.5 and 1 Hz. For the measurements in liquid, a drop of buffer was deposited directly on the sample surface and immediately scanned. The time of analysis was short enough to avoid major liquid evaporation. Semi-contact silicon cantilever (HQ:NSC15; Mikromash) with a spring constant of 40 N m^{-1} was used. Surface topography was acquired by height channel. Images were processed with the manual tilt correction of the software SPIP (ImageMet). Wettability measurements were performed by a contact angle system OCA 15 from Dataphysics. A series of sessile water droplets of 2 µL deposited at the surface of each sample by means of a syringe pump were realized. The value of the static WCA was extracted from the droplet shape using a numerical fit based on the Laplace–Young model. A series of three droplets were deposited at different locations on the sample in order to obtain an average value.

Biomolecule Grafting: The plasma-polymerized layers on SS discs and etched titanium were sterilized by UV irradiation, then under laminar flow were immersed in 1 mg mL^{-1} of DispB (42 kDa) in PBS [10×10^{-3} m] solutions at pH 7.2 and left for 1 h under gentle agitation at room temperature. Afterward, the samples were subjected to thorough cleaning with PBS buffer in order to remove unbounded enzyme, and blow-dried with nitrogen before their use on biological assays. PDA layers were immersed in DispB and cleaned in same conditions.

Antibiofilm Activity Assessment: A preculture *of S. epidermidis* (ATCC35984) was grown until reaching optical density of 0.6. Then the culture was diluted tenfold in M63 medium (Sigma Aldrich) and disc samples were inoculated with 200 µL of the bacteria solution and incubated at 37 °C for 24 h. Nonadherent bacteria were removed by rinsing with sterilized deionized water and adherent biofilm bacteria were recovered via abrasion over glass beads for 10 min after 500-fold dilution in LB medium and 3 min sonication to resuspend adherent bacteria. Recovered bacteria were incubated in dilutions up to 4× overnight on LB agar in plates at 37 °C, followed by colony-forming units counting. For each layer, six replicates were used, three of them to calculate the total number of bacteria on the surface of the sample and the other three to determine the adherent bacteria.

Cell Viability and Adhesion Properties: All manipulations were made under sterile conditions (L2 laminar flow hood). The cells were cultured under the condition of 5% CO_2 and 37 °C (Binder incubator, Tuttlingen, Germany). Twelve well black plates with lid (p12-1.5H-N, In Vitro Scientific) adapted to SS size (20 mm) were used and polystyrene culture wells (CD) were seeded as reference positive control.

Published in : Advanced Science News (2018), 1701059
DOI: 10.1002/adhm.201701059
Status : Postprint (Author's version)

Three sample discs were prepared for each condition and experiment was made in two replicates (one passage between the two replicates). All wells were rinsed with 1 mL physiological PBS solution, then 1 mL complete culture medium, and incubated 30 min at CO_2 incubator. Complete medium was Dulbecco's Modified Eagle Medium DMEM high glucose, GlutaMAX Supplement, pyruvate (31966-021 Gibco, Invitrogen, Paisley, UK) supplemented with 10% inactivated fetal bovine serum (Gibco), 100 IU mL^{-1} penicillin-100 µg mL^{-1} streptomycin (Lonza, Verviers, Belgium). The 10 000 MG-63 (mycoplasma-free) cell lines were seeded per well in 1 mL complete medium.

To evaluate the living cell population on the different conditions, a viability test was then performed directly on discs at 72 h. Cellular viability of 100% was attributed to the MG-63 grown on plasma-cleaned SS. Supplementary control (PS) wells without disc samples were also added to verify seeding and growth until 72 h on bright field inverted microscope. Cellular viability was quantified by a colorimetric assay using 3-(4,5-dimethylthiazol-2-yl)-5-(3-carboxymethoxyphenyl)-2-(4-sulfophenyl)2H-tetrazolium (inner salt MTS, Promega, Madison, USA). MTS solutions were prepared according to the manufacturer's instructions. Discs were rinsed with 1 mL of DMEM/F-12 (Gibco) and 1 mL of new DMEM/F-12 with MTS solution (10%) was applied. The plates were incubated at 37 °C in the absence of light for 45 min. Following this, the plates were shaken for 3 min. A 200 µL of supernatant was removed from each well and placed in 96 well microplates. The absorbance of supernatant aliquots was read at 492 nm using the Powerwave X microplate spectrophotometer (Biotek instrument Inc., Winooski, VT, USA), and the viability was calculated and normalized from the absorbance of control samples taken as 100% (plasma cleaned SS, WCA: 32°). Immunofluorescence staining was conducted after the MTS assays. Discs were rinsed two times with 1 mL PBS, and the cells were fixed with 4% paraformaldehyde (SigmaAldrich) in PBS at room temperature for 20 min. An immuno-staining was then performed and the number of cells, their covering on discs, and their morphology were determined from microscopic fluorescent images. Cell permeabilization was performed with 1 mL 0.5% Triton X-100 (Sigma) at 4 °C for 20 min. Blocking was performed with 1% BSA (Sigma) in PBS at 37 °C for 30 min. Vinculin was stained with mouse anti-vinculin (Sigma Aldrich V9131) and rabbit anti-mouse alexa fluor 568 (Life Technologies, Carlsbad, California, United States), the incubation was performed in PBS solution with corresponding dilutions (1:200), at 37 °C for 1 h for mouse anti-vinculin and at room temperature or 30 min for rabbit antimouse alexa fluor 568. Actin was stained by incubating in PBS solution with 1:40 dilution of Alexa fluor 488-labeled phalloidin (Life Technologies) at 37 °C for 1 h. A nuclear stain dye DAPI (D8417-1MG, Sigma)/PBS 1:5000 was added and allowed to set in at room temperature for 10 min. The stained sample surface was imaged with an IX81 optical inverted microscope equipped with a UPlanFL objective at 10× magnification and with an XCite-iris IX fluorescence unit and a C-BUN-FXC50 charge-coupled-device camera (Olympus Optical Co., Ltd.). An image analysis software "CellSens" (Olympus) was used to quantify the number of cells and their coverage on discs. Panorama (10× magnification) per sample was performed to allow the analysis of the entire disc surface. For surface occupancy and cell spreading, 100% of surface corresponds to disc surface (3.1417 cm^2). A qualitative analysis of cellular morphology on discs was conducted with the fluorescent actin, DAPI, and vinculin staining at 72 h with a 20× magnification (immersion oil objective). Light Sheet microscope Airyscan processing was also used for visualization of vinculin at focal points. For etched titanium discs, similar experiments were realized, but reducing by half all

solutions to adapt to the smaller size of the 48 well plates adapted to the titanium discs size (⦰ 10 mm) (here seeding of 5000 MG-63 in 0.5 mL complete medium).

Statistical Analysis: Wilcoxon–Mann–Whitney test was used for mean comparison using R i386 3.3.0 software; means ± standard errors were calculated; $n = 6$; P value < 1% (very significant). See the Supporting Information for the complete data set.

Supporting Information

Supporting Information is available from the Wiley Online Library or from the author.

Acknowledgements

This research was carried out in the framework of the European M-ERA. NET METABIO project funded by the Luxembourgish Agency "Fonds National de la Recherche" (FNR-INTERMAT/13/13) and the DG06Region Wallonne Agency (No. convention 1318213). The authors would like to thank J. Guillot, J-L. Biaggi, S. Cambier, P. Grysan, T. Gaulain, and N. Valle from LIST for their skillful characterization and valuable discussions. S. Smeets and F. Cambroisier were funded by METABIO for cell culture studies (University of Liege). C.D. is F.R.R-FNRS Research Director and thanks FNRS for financial support.

Conflict of Interest

The authors declare no conflict of interest.

[1] a) J. Raphel, M. Holodniy, S. B. Goodman, S. C. Heilshorn, *Biomaterials* **2016**, *84*, 301; b) J. Raphel, J. Karlsson, S. Galli, A. Wennerberg, C. Lindsay, M. G. Haugh, J. Pajarinen, S. B. Goodman, R. Jimbo, M. Andersson, S. C. Heilshorn, *Biomaterials* **2016**, *83*, 269; c) T. Zhou, Y. Zhu, X. Li, X. Liu, K. W. K. Yeung, S. Wu, X. Wang, Z. Cui, X. Yang, P. K. Chu, *Prog. Mater. Sci.* **2016**, *83*, 191; d) B. G. Zhang, D. E. Myers, G. G. Wallace, M. Brandt, P. F. Choong, *Int. J. Mol. Sci.* **2014**, *15*, 11878.

[2] B. Brena, P. González-Pombo, F. Batista-Viera, in *Immobilization of Enzymes and Cells*, 3rd ed. (Ed: J. M. Guisan), Humana Press, Totowa, NJ **2013**, p. 15.

[3] a) M. Liu, G. Zeng, K. Wang, Q. Wan, L. Tao, X. Zhang, Y. Wei, *Nanoscale* **2016**, *8*, 16819; b) X. Yu, J. Walsh, M. Wei, *RSC Adv.* **2013**, *4*, 7185; c) C. K. Poh, Z. Shi, T. Y. Lim, K. G. Neoh, W. Wang, *Biomaterials* **2010**, *31*, 1578.

[4] H. Lee, S. M. Dellatore, W. M. Miller, P. B. Messersmith, *Science* **2007**, *318*, 426.

[5] a) H. Lee, J. Rho, P. B. Messersmith, *Adv. Mater.* **2009**, *21*, 431; b) Q. Ye, F. Zhou, W. Liu, *Chem. Soc. Rev.* **2011**, *40*, 4244; c) M. Corno, M. Delle Piane, P. Choquet, P. Ugliengo, *Phys. Chem. Chem. Phys.* **2017**, *19*, 7793.

[6] E. Faure, C. Falentin-Daudré, C. Jérôme, J. Lyskawa, D. Fournier, P. Woisel, C. Detrembleur, *Prog. Polym. Sci.* **2013**, *38*, 236.

[7] a) E. J. Szili, R. D. Short, D. A. Steele, J. W. Bradley, in *Surface Modification of Biomaterials*, Woodhead Publishing, Sawston, Cambridge, UK **2011**, p. 3; b) K. S. Siow, L. Britcher, S. Kumar, H. J. Griesser, *Plasma Processes Polym.* **2006**, *3*, 392; c) J. Buxadera-Palomero, C. Canal, S. Torrent-Camarero, B. Garrido, F. J. Javier Gil, D. Rodríguez, *Biointerphases* **2015**, *10*, 029505.

[8] a) C. Hoffmann, C. Berganza, J. Zhang, *Med. Gas Res.* **2013**, *3*, 21; b) P. Bourke, D. Ziuzina, L. Han, P. J. Cullen, B. F. Gilmore, *J. Appl. Microbiol.* **2017**, *123*, 308; c) Z. Chen, H. Simonyan, X. Cheng, E. Gjika, L. Lin, J. Canady, J. Sherman, C. Young, Keidar, *Cancers* **2017**, *9*, 61.

[9] a) A. Cunha, R. P. Renz, E. Blando, R. B. de Oliveira, R. Hübler, *J. Biomed. Mater. Res., Part A* **2014**, *102*, 30; b) F. Rezaei, B. Shokri, Sharifian, *Appl. Surf. Sci.* **2016**, *360*, 641.

[10] Y. Yin, S. G. Wise, N. J. Nosworthy, A. Waterhouse, D. V. Bax, H. Youssef, M. J. Byrom, M. M. Bilek, D. R. McKenzie, A. S. Weiss, K. Ng, *Biomaterials* **2009**, *30*, 1675.

[11] a) F. Harding, R. Goreham, R. Short, K. Vasilev, N. H. Voelcker, *Adv. Healthcare Mater.* **2013**, *2*, 585; b) R. Mauchauffé, S. Bonot, M. Moreno-Couranjou, C. Detrembleur, N. D. Boscher, C. Van De Weerdt, A.-S. Duwez, P. Choquet, *Adv. Mater. Interfaces* **2016**, *3*, 1500520; c) G. Camporeale, M. Moreno-Couranjou, S. Bonot, R. Mauchauffé, N. D. Boscher, C. Bebrone, C. Van de Weerdt, H.-M. Cauchie, P. Favia, P. Choquet, *Plasma Processes Polym.* **2015**, *12*, 1208.

[12] a) R. Mauchauffé, M. Moreno-Couranjou, N. D. Boscher, A.-S. Duwez, P. Choquet, *Plasma Processes Polym.* **2016**, *13*, 843; b) R. Mauchauffé, M. Moreno-Couranjou, N. D. Boscher, C. Van De Weerdt, A.-S. Duwez, P. Choquet, *J. Mater. Chem. B* **2014**, *2*, 5168; c) M. Moreno-Couranjou, R. Mauchauffé, S. Bonot, C. Detrembleur, P. Choquet, *J. Mater. Chem. B* **2018**, *6*, 614.

[13] M. Chen, Q. Yu, H. Sun, *Int. J. Mol. Sci.* **2013**, *14*, 18488.

[14] a) M. Otto, *Annu. Rev. Med.* **2013**, *64*, 175; b) F. Valour, S. Trouillet-Assant, J. P. Rasigade, S. Lustig, E. Chanard, H. Meugnier, S. Tigaud, F. Vandenesch, J. Etienne, T. Ferry, F. Laurent, B. J. I. S. G. Lyon, *PLoS One* **2013**, *8*, e67240.

[15] a) C. R. Arciola, D. Campoccia, P. Speziale, L. Montanaro, W. Costerton, *Biomaterials* **2012**, *33*, 5967; b) J. L. Lister, A. R. Horswill, *Front. Cell. Infect. Microbiol.* **2014**, *4*, 178.

[16] a) N. Ramasubbu, L. M. Thomas, C. Ragunath, J. B. Kaplan, *Mol. Biol.* **2005**, *349*, 475; b) M. Kostakioti, M. Hadjifrangiskou, S. J. Hultgren, *Cold Spring Harbor Perspect. Med.* **2013**, *3*, a010306; c) A. Gokcen, A. Vilcinskas, J. Wiesner, *Virulence* **2013**, *4*, 260.

[17] G. Donelli, I. Francolini, D. Romoli, E. Guaglianone, A. Piozzi, C. Ragunath, J. B. Kaplan, *Antimicrob. Agents Chemother.* **2007**, *51*, 2733.

[18] E. Faure, C. Falentin-Daudré, T. S. Lanero, C. Vreuls, G. Zocchi, C. Van De Weerdt, J. Martial, C. Jérôme, A.-S. Duwez, C. Detrembleur, *Adv. Funct. Mater.* **2012**, *22*, 5271.

[19] X. Miao, D. Wang, L. Xu, J. Wang, D. Zeng, S. Lin, C. Huang, X. Liu, X. Jiang, *Int. J. Nanomed.* **2017**, *12*, 1415.

[20] M. Øilo, V. Bakken, *Materials* **2015**, *8*, 2887.

[21] a) L. Le Guehennec, M. A. Lopez-Heredia, B. Enkel, P. Weiss, Y. Amouriq, P. Layrolle, *Acta Biomater.* **2008**, *4*, 535; b) K. Anselme, *Biomaterials* **2000**, *21*, 667.

[22] a) L. Treccani, T. Yvonne Klein, F. Meder, K. Pardun, K. Rezwan, *Acta Biomater.* **2013**, *9*, 7115; b) L. Chen, J. Hu, J. Ran, X. Shen, H. Tong, *RSC Adv.* **2015**, *5*, 56410.

[23] N. Shams, M. Ghasemi, S. Sadatmansouri, S. Bonakdar, *J. Dent. Tehran Univ. Med. Sci.* **2015**, *12*, 424.

[24] a) C. P. Quinn, C. P. Pathak, A. Heller, J. A. Hubbell, *Biomaterials* **1995**, *16*, 389; b) J. A. Killion, L. M. Geever, D. M. Devine, J. E. Kennedy, C. L. Higginbotham, *J. Mech. Behav. Biomed. Mater.* **2011**, *4*, 1219.

[25] a) A. Charlot, V. Sciannaméa, S. Lenoir, E. Faure, R. Jérôme, C. Jérôme, C. Van De Weerdt, J. Martial, C. Archambeau, N. Willet, A.-S. Duwez, C.-A. Fustin, C. Detrembleur, *J. Mater. Chem.* **2009**, *19*, 4117; b) N. Patil, C. Falentin-Daudré, C. Jérôme, C. Detrembleur, *Polym. Chem.* **2015**, *6*, 2919; c) S. H. Ku, C. B. Park, *Adv. Healthcare Mater.* **2013**, *2*, 1445; d) Z. Yang, Q. Tu, Y. Zhu, R. Luo, X. Li, Y. Xie, M. F. Maitz, J. Wang, N. Huang, *Adv. Healthcare Mater.* **2012**, *1*, 548.

[26] T.-C. Tsai, D. Staack, *Plasma Processes Polym.* **2011**, *8*, 523.

[27] a) T. B. Casserly, K. K. Gleason, *Chem. Vap. Deposition* **2006**, *12*, 59; b) T. P. Kasih, S.-i. Kuroda, H. Kubota, *Plasma Processes Polym.* **2007**, *4*, 648.

[28] L. Sangely, B. Boyer, E. de Chambost, N. Valle, J.-N. Audinot, T. Ireland, M. Wiedenbeck, J. Aleon, H. Jungnickel, J.-P. Barnes, P. Bienvenu, U. Breuer, *Sector Field Mass Spectrometry for Elemental and Isotopic Analysis*, The Royal Society of Chemistry, Cambridge, UK **2015**, p. 439.

[29] A. Han, X. Li, B. Huang, J. K. H. Tsoi, J. P. Matinlinna, Z. Chen, D. M. Deng, *Int. J. Adhes. Adhes.* **2016**, *69*, 125.

[30] M. E. Lynge, R. van der Westen, A. Postma, B. Stadler, *Nanoscale* **2011**, *3*, 4916.

[31] A. Liu, L. Zhao, H. Bai, H. Zhao, X. Xing, G. Shi, *ACS Appl. Mater. Interfaces* **2009**, *1*, 951.

[32] J. M. Anderson, in *An Introduction to Biomaterials* (Eds: A. G. Scott, J. O. Hollinger) CRC Press, FL, USA **2006**, Ch. 3, p. 3.

[33] M. Keremidarska, E. Radeva, K. Eleršicˇ, A. Iglicˇ, L. Pramatarova, N. Krasteva, *J. Phys.: Conf. Ser.* **2014**, *558*, 012057.

[34] a) T.-T. Yu, F.-Z. Cui, Q.-Y. Meng, J. Wang, D.-C. Wu, J. Zhang, X.-X. Kou, R.-L. Yang, Y. Liu, Y. S. Zhang, F. Yang, Y.-H. Zhou, *ACS Biomater. Sci. Eng.* **2017**, *3*, 1119; b) P. C. Schamberger, J. A. Gardella, *Colloids Surf., B* **1994**, *2*, 209.

[35] T. Wassmann, S. Kreis, M. Behr, R. Buergers, *Int. J. Implant Dent.* **2017**, *3*, 32.

[36] B. Groessner-Schreiber, R. S. Tuan, *J. Cell Sci.* **1992**, *101*, 209.

[37] C. Grenade, M. C. De Pauw-Gillet, C. Pirard, V. Bertrand, C. Charlier, A. Vanheusden, A. Mainjot, *Dent. Mater.* **2017**, *33*, 333.